HEPATOBILIARY-PANCREAS

CrossMark

CT diagnosis of gallbladder adenomyomatosis: importance of enhancing mucosal epithelium, the "cotton ball sign"

Hyun Kyung Yang [1,2] · Jeong Min Lee [1,3] (ID) · Mi Hye Yu [4] · Sang Min Lee [5] · Jinyoung Park [6] · Na Young Han [7] · Kyoungbun Lee [8] · Jin-Young Jang [9] · Joon Koo Han [1,3]

ABSTRACT

Objectives To determine the diagnostic value of the cotton ball sign and other CT features in patients with gallbladder (GB) wall thickenings (WTs).

Methods Three blinded readers reviewed the preoperative CT and MR images of 101 patients with pathologically confirmed GB adenomyomatosis (GA) ($n = 34$) and other benign ($n = 29$), malignant ($n = 41$), and premalignant ($n = 2$) GBWTs. Three readers analysed the morphological features of GBWT and presence of the "cotton ball sign", defined as fuzzy grey dots in GBWT or a dotted outer border of the inner enhancing layer on contrast-enhanced (CE) CT. In addition, the "pearl necklace sign" on MR was analysed.

Results In the GA group ($n = 34$), prevalence of the cotton ball sign and pearl necklace sign was 74% (25/34) and 44% (15/34), respectively. Presence of the cotton ball sign, smooth contour of the mucosa, double-layering enhancement, and enhancement degree weaker than the renal cortex on CT images were significant predictors of benign GBWT ($p < 0.01$). When differentiating GA from GB malignancy or premalignancy, accuracy of the cotton ball sign and pearl necklace sign was 81% (62/77) and 74% (57/77), respectively.

Conclusion The cotton ball sign on CE-CT showed higher sensitivity and comparable specificity to those of the pearl necklace sign in differentiating GA from malignancy.

Key Points
• *Prevalence of the cotton ball sign on CT was 74% in gallbladder adenomyomatosis.*
• *The cotton ball sign was useful in differentiating gallbladder adenomyomatosis from gallbladder cancer.*
• *The cotton ball sign was more sensitive than the pearl necklace sign for adenomyomatosis diagnosis.*

Keywords Gallbladder diseases · Adenomyoma · Gallbladder neoplasms · Diagnosis, differential · Tomography, X-ray computed

✉ Jeong Min Lee
jmsh@snu.ac.kr

1 Department of Radiology, Seoul National University Hospital, 101 Daehak-ro, Jongno-gu, Seoul 03080, Korea

2 The Joint Department of Medical Imaging, Mount Sinai Hospital-University Health Network-Women's College Hospital, University of Toronto, Toronto, ON, Canada

3 Department of Radiology, Seoul National University College of Medicine, Seoul, Korea

4 Department of Radiology, Konkuk University School of Medicine, Seoul, Korea

5 Department of Radiology, Hallym University Sacred Heart Hospital, Anyang, Gyeonggi-do, Korea

6 Department of Radiology, Dongnam Institute of Radiological and Medical Sciences, Busan, Korea

7 Department of Pathology, National Cancer Center, Goyang, Gyeonggi-do, Korea

8 Department of Pathology, Seoul National University Hospital, Seoul, Korea

9 Department of Surgery, Seoul National University Hospital, Seoul, Korea

Abbreviations

CE   Contrast enhanced
CT   Computed tomography
GA   Gallbladder adenomyomatosis
GB   Gallbladder
GBWT   Gallbladder wall thickening
GRE   Gradient echo sequence
HU   Hounsfield unit
MDCT   Multi-detector computed tomography
MRCP   Magnetic resonance cholangiopancreatography
MRI   Magnetic resonance imaging
PVP   Portal venous phase
RAS   Rokitansky-Aschoff sinus
US   Ultrasound

Introduction

Gallbladder adenomyomatosis (GA) is a common benign entity presenting as an asymptomatic gallbladder (GB) mass or wall thickening (WT), diagnosed in 2%–9% of all cholecystectomies [1, 2]. GA is characterised pathologically by excessive proliferation of the surface epithelium and hypertrophy of the muscularis propria. With invagination of the mucosa into the thickened muscularis, Rokitansky-Aschoff sinuses (RAS) with crystal precipitation and calcification can develop from progressive concentration of bile [3, 4]. The radiological evidence of both GA and GB cancer is focal or diffuse thickening of the GB wall. Preoperative differentiation between them is critical to avoid unnecessary cholecystectomies in patients with GA [3]. Furthermore, given its relatively high prevalence and the continuous improvement in the performance of ultrasound (US) and computed tomography (CT), GA can be more frequently encountered during everyday practice, warranting the need for better differentiation [2, 3, 5].

Transabdominal US is the imaging modality of choice for diagnosing GA and enables correct identification and characterisation of GA in many cases [3]. A previous study from Asia reported that US using high-frequency probes and precise focal depth adjustment provided accuracy values ranging from 91.5 to 94.8% in differentiating GA from early-stage GB cancer [6]. However, in actual practice, there is a limitation to transabdominal US in that the GB wall is sometimes poorly visible via the classical sub-costal approach, particularly because of obesity or interposition of the bowel between the abdominal wall and the GB wall. Particularly, the GB fundal wall is sometimes difficult to examine because of reverberation artefacts [7, 8].

In several studies using various imaging modalities [9–13] conducted to provide a more precise preoperative diagnosis for gallbladder wall thickening (GBWT), findings of cyst-like spaces in a thickened GB wall have been demonstrated to indicate GA. This is called the pearl necklace sign on MRI,

referring to small, rounded, high-signal intensity foci within the GBWT on T2-weighted image (T2WI) that correspond to bile-filled RAS [10, 11, 14] and the rosary sign on CT, i.e., round cystic spaces lined by enhancing epithelium within the unenhanced, hypertrophied muscular layer of the GB wall [15–18]. However, according to a previous study [11], CT showed limited sensitivity of 24% in diagnosing GA using the presence of small calcifications or RAS, and the pearl necklace sign on MRCP also showed limited sensitivity of 62%. Hence, preoperative differentiation between benign and malignant GBWTs still remains an important dilemma for radiologists [3]. Although radiological diagnosis is largely dependent on visualising RAS, only RAS of sufficient size can be visualised on imaging studies. In cases of GA in which RAS is smaller than 3 mm or filled with biliary sludge or calculi, the pearl necklace sign and rosary sign are sometimes not evident [18, 19]. So, instead, we hypothesised that in GA with small or collapsed RAS, epithelial proliferation lining RAS may be a clue in diagnosing GA, seen as fuzzy grey enhancing dots in a thickened GB wall or a dotted outer border of an inner enhancing layer of the GB wall on contrast-enhanced (CE) CT, referred to as the "cotton ball sign". This idea was suggested from our experience; when inspecting the histology slides of adenomyomatosis cases, in a case of adenomyomatosis that showed the cotton ball sign without evident cystic spaces on CT, we noted multiple RAS smaller than 2 mm including at least one RAS containing bile. In contrast, in a case of adenomyomatosis showing multiple cystic spaces and their lining enhancing epithelia visible on CT images correlating with pearl necklace sign on MR T2WI, we noticed multiple RAS exceeding 2 mm.

Therefore, we conducted this study to determine the diagnostic performance of the cotton ball sign along with several other imaging features on CT in patients with pathologically proven GB diseases that show diffuse or focal GBWT.

Materials and methods

Study population

Our Institutional Review Board approved this retrospective study and waived the requirement for written informed consent. We performed a retrospective consecutive computerised search of the electronic medical records at our institution for patients who underwent cholecystectomy for suspected GB diseases between January 2006 and December 2015 and obtained their preoperative CT and MR examinations. From the search, we found 194 patients. Inclusion criteria were as follows: (1) available histological diagnosis of the cholecystectomy specimen, (2) available preoperative CE-CT and preoperative CE-MR, and (3) focal or diffuse GBWT ≥ 3 mm [9, 20–23] on preoperative CT. GB wall of ≥ 3 mm thickness was

defined to be GBWT according to the previous literatures [9, 20]. Exclusion criteria were as follows: a lack of preoperative CE-CT ($n = 1$); a lack of preoperative CE-MR ($n = 3$); suboptimal image quality due to artefacts ($n = 1$); GB-replacing masses ($n = 2$); GB masses or WTs invading adjacent structures ($n = 6$); polyps or polypoid masses protruding into the GB lumen ($n = 46$); papillary lesions ($n = 7$); underlying disease not directly related to GBWT (choledochal cyst) ($n = 1$); no definite GBWT on CT ($n = 26$). Finally, 101 patients [mean age, 62 years (range, 24–85 years); 55 males (mean age, 61 years; range, 24–82 years), and 46 females (mean age, 63 years; range, 38–85 years)] with 106 focal or diffuse GBWT lesions were enrolled in our study. Ninety-six GBWTs were observed in 96 patients, i.e., a single GBWT per patient. The remaining ten focal GBWTs were observed in five patients, i.e., two GBWTs per patient (Fig. 1). The time interval between preoperative CT/MR imaging and cholecystectomy ranged from 0 to 89 days.

Histopathological diagnosis of the cholecystectomy specimen served as the reference standard of each GBWT. Histopathological preparation for the cholecystectomy specimen was done as follows. The gallbladder was opened lengthwise through its serosa-lined surface. Beginning at the fundus, a cut was made through the body and neck of the gallbladder and then through the cystic duct [24]. Entire tumours were mapped if found. Even when tumours were not obviously identified or the preoperative diagnosis did not favour malignancy, the entire specimens were embedded when the gallbladder wall was ≥

3 mm thick and firm. Among the 106 GBWTs, 63 lesions were pathologically confirmed as benign, 41 lesions were malignant, and 2 were premalignant. The benign GBWT group was divided into GAs and other benign GBWTs. GBWTs diagnosed with "adenomyomatous hyperplasia", characterised by excessive proliferation of the surface epithelium and hypertrophy of the muscularis propria, with RAS on histopathological examination, were categorised as definite GA [2, 5]. When there was proliferation of the surface epithelium and RAS in the muscle layer of the GB without severe hypertrophy of the muscle component on histopathological examination, we categorised them as mild GA. Definite ($n = 24$) and mild ($n = 10$) GAs comprised the GA group of our study. Twenty-nine benign GBWTs with neither adenomyomatous hyperplasia nor RAS were categorised as the other benign group. Forty-one pathologically confirmed malignant GBWTs and two pathologically confirmed premalignant GBWTs comprised the malignant or premalignant group (Fig. 1).

CT image acquisition

Seventy-three patients included in our study underwent CT at our institution on an MDCT scanner. Seventy patients underwent one of the following CT scans: quadruple-phase CT ($n = 64$) consisting of unenhanced, early arterial, late arterial, and portal venous phases; quadruple-phase CT ($n = 1$) consisting of unenhanced, late arterial, portal venous, and delayed phases; or triple-phase CT ($n = 5$) consisting of unenhanced, late arterial,

Fig. 1 Flowchart showing the patient selection process
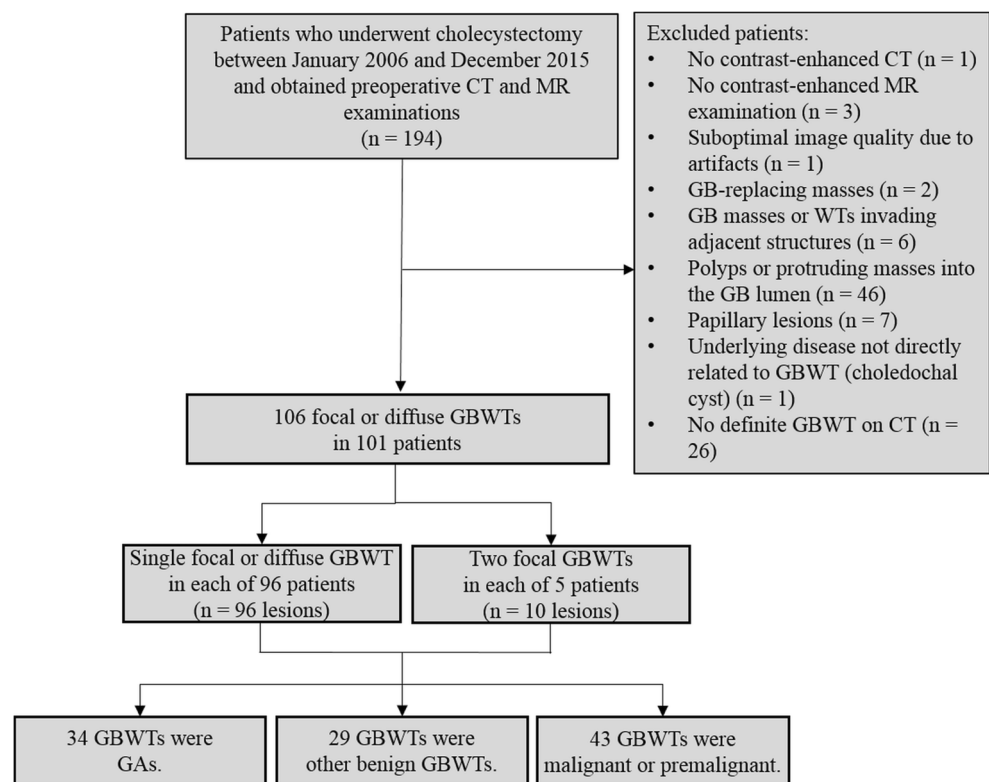
and portal venous phases. The remaining three patients underwent either triple-phase CT ($n = 1$) consisting of late arterial, portal venous, and delayed phases or single phase CT ($n = 2$) consisting of the portal venous phase. Details of imaging techniques are provided in the Supplementary Material. The remaining 28 patients underwent CT at an outside hospital. They all included the unenhanced and portal venous phase scans.

MR image acquisition

Ninety-seven patients included in our study underwent MR examination at our institution. Detailed techniques of MR imaging are provided in the Supplementary Material. The remaining four patients included in our study underwent MR examinations at an outside hospital.

Image analysis

Three abdominal imaging radiologists (M.H.Y, S.M.L, and J.P. who had 10, 8, and 5 years in the interpretation of body CT and MR images, respectively) independently evaluated the CT and MR images on a picture-archiving and communication system workstation in two separate review sessions, with a washout period of 2 weeks to reduce recall bias (CT in the first session and MR imaging in the second session). The readers were aware of the study design and knew that patients had a diagnosis of either benign or malignant GBWT, but were blinded to the specific pathological diagnosis of each case. For five patients who had co-existing separate focal WTs, we informed the readers of the specific location (e.g., fundus, body, or neck) of each lesion.
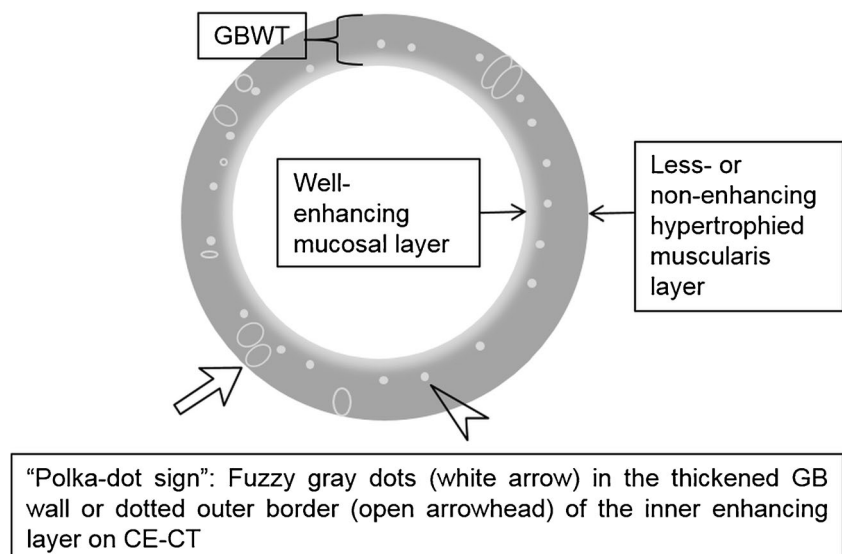
Before reviewing the images, we provided instructions describing the concept of the cotton ball sign using a schematic diagram (Fig. 2) and illustrative cases of positive and negative

cotton ball signs to each reader. The cotton ball sign was defined as fuzzy grey enhancing dots in a thickened GB wall or a dotted outer border of an inner enhancing layer of the GB wall on CE-CT. The readers rated the presence of the cotton ball sign on the following five-point scale: 1, definitely absent; 2, probably absent; 3, indeterminate; 4, probably present; 5, definitely present. Ratings were dichotomised such that the cotton ball sign was present at a rating of 4 or 5 and considered absent at lower ratings. The threshold was based on the rationale that such a decision reflects the real practice, wherein surgeons have to decide whether or not to perform surgery. The readers also assessed the following findings of the GBWTs by reviewing the CT images [1]: (1) mucosal smoothness (smooth vs. irregular) and (2) layered pattern (double layer vs. single layer) on portal venous images; when GBWT showed a more strongly enhancing inner layer and weakly enhancing or non-enhancing outer layer, it was categorised as a double layer pattern, and when GBWT could not be described as outer and inner layers of different enhancement degrees, it was categorised as a single layer pattern. (3) The enhancement degree (weaker than the renal cortex, similar to or stronger than the renal cortex) on portal venous images and (d) pericholecystic infiltration (present vs. absent) were assessed. They also controlled for the presence of the pearl necklace sign on MRI, defined as small round foci with the same markedly high signal intensity as bile within the GBWT on T2WI or MRCP [11].

Statistical analysis

We determined the presence or absence of each imaging feature based on the interpretations of two (S.M.L. and J.P.) of the three readers. In cases of discrepancy, we used the interpretation of the other reader (M.H.Y.). Inter-observer agreement for

Fig. 2 Schematic diagram of the cotton ball sign. GBWT = gallbladder wall thickening; GB = gallbladder; CE-CT = contrast-enhanced computed tomography

GBWT

Well-enhancing mucosal layer

Less- or non-enhancing hypertrophied muscularis layer

"Polka-dot sign": Fuzzy gray dots (white arrow) in the thickened GB wall or dotted outer border (open arrowhead) of the inner enhancing layer on CE-CT

each imaging feature was analysed using kappa statistics and was interpreted as follows: poor, < 0.20; fair, 0.20–0.39; moderate, 0.40–0.59; substantial, 0.60–0.79; almost perfect, ≥ 0.80 [19]. Prevalence of the cotton ball sign and pearl necklace sign in each group (GA group, other benign group, and malignant or premalignant group) were calculated. We used the chi-square test to compare the prevalence of the cotton ball sign in each group. Thereafter, the sensitivity, specificity, and accuracy of the cotton ball sign and pearl necklace sign in differentiating between the GA group and malignant or premalignant group were calculated. McNemar's test was used to compare the sensitivity and specificity of the cotton ball sign and pearl necklace sign.

Imaging features were compared between the benign and malignant or premalignant groups using the Fisher's exact test for categorical variables. All analysis was done on the per-lesion basis. The potential clustering effect of ten GBWTs observed in five patients was considered to be minor and ignored. Multivariate logistic regression analysis was performed to find the most predictive CT finding. All statistical analyses were performed using MedCalc software v. 14.12.0 (Mariakerke, Belgium) and SPSS v. 19.0 (New York, US). We considered a two-tailed p value < 0.05 to indicate statistical significance.

Results

Cotton ball sign on CT and pearl necklace sign on T2WI and MRCP

The cotton ball sign was present in 74% (25/34) of the GA group (Figs. 3 and 4). The pearl necklace sign was present in 44% (15/34) of the GA group (Table 1). When differentiating GA from GB malignancy or premalignancy, the cotton ball sign showed significantly higher sensitivity (74%, 25/34) than the pearl necklace sign (44%, 15/34) (p < 0.05, Fig. 3), but did not show a significant difference in terms of specificity (86%, 37/43 vs. 98%, 42/43, p = 0.06) (Table 2). The sensitivity, specificity, and accuracy of the pearl necklace sign in differentiating GA from malignancy or premalignancy in cases scanned by 1.5-T magnets were 43% (6/14), 100% (10/10), and 67% (16/24), respectively. In cases scanned by 3.0-T magnets, they were 45% (9/20), 97% (32/33), and 77% (41/53), respectively. No statistical difference was found between the performance of the 1.5-T group and that of the 3.0-T group. In addition, the three readers showed fair to moderate agreements for the cotton ball sign (0.39–0.56) and substantial to almost perfect agreements for the pearl necklace sign (0.65–0.84).
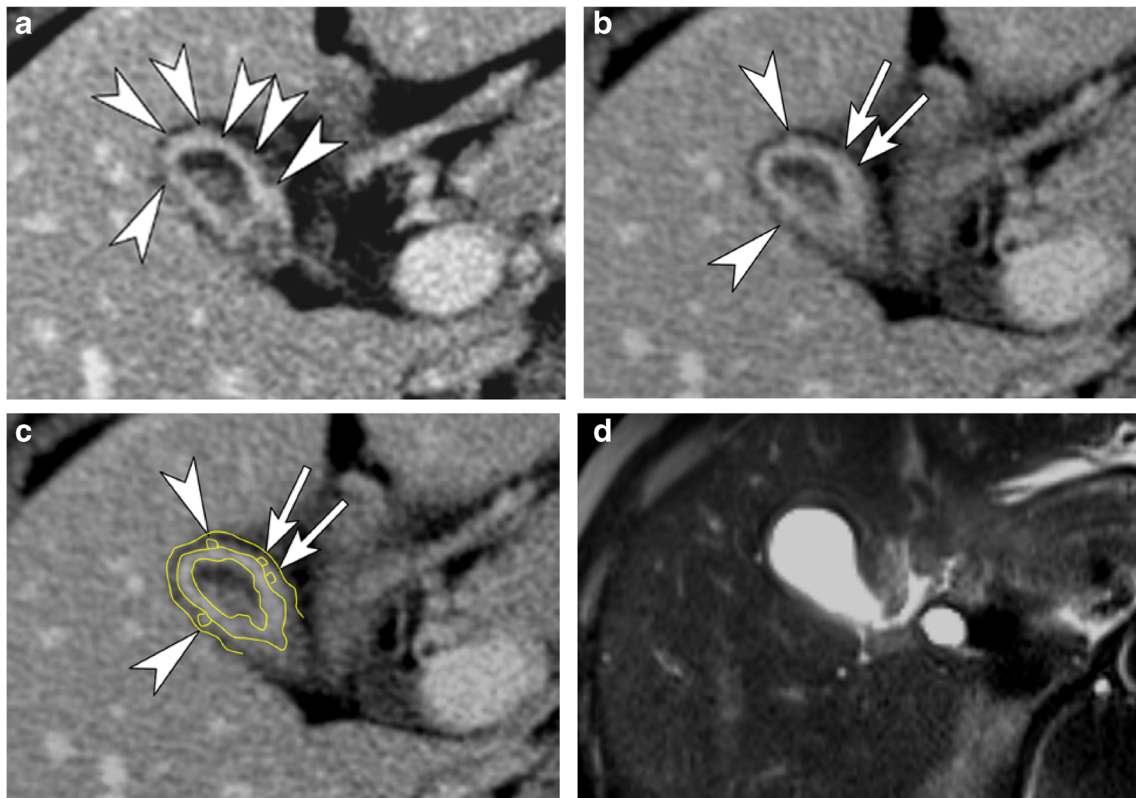

Fig. 3 A 50-year-old male, pathologically proven GA with a positive cotton ball sign on CT and negative pearl necklace sign on T2WI. **A**, **B**, **C** Portal venous phase CT images show diffuse thickening of the gallbladder wall with internal several fuzzy grey dots (*arrows*) and a dotted outer border (*arrowheads*), "cotton ball sign". In addition, double layer enhancement was noted in the diffuse GBWT. In **C**, yellow guides were added to **B** to aid following the annotations. **D** On T2WI of the same patient, the pearl necklace sign is not noted. GA = gallbladder adenomyomatosis; GBWT = gallbladder wall thickening

Fig. 4 A 56-year-old female, pathologically proven GA with a positive cotton ball sign on CT and positive pearl necklace sign on T2WI. **A**, **B**, **C** Portal venous phase transverse CT images show focal thickening of the GB wall with internal several fuzzy grey dots (*arrows*) and a dotted outer border (*arrowheads*), "cotton ball sign". On **C**, yellow guides were added to **B** to aid following the annotations. **D** On T2WI of the same patient, the pearl necklace sign (*curved arrow*) is noted. GA = gallbladder adenomyomatosis; GB = gallbladder
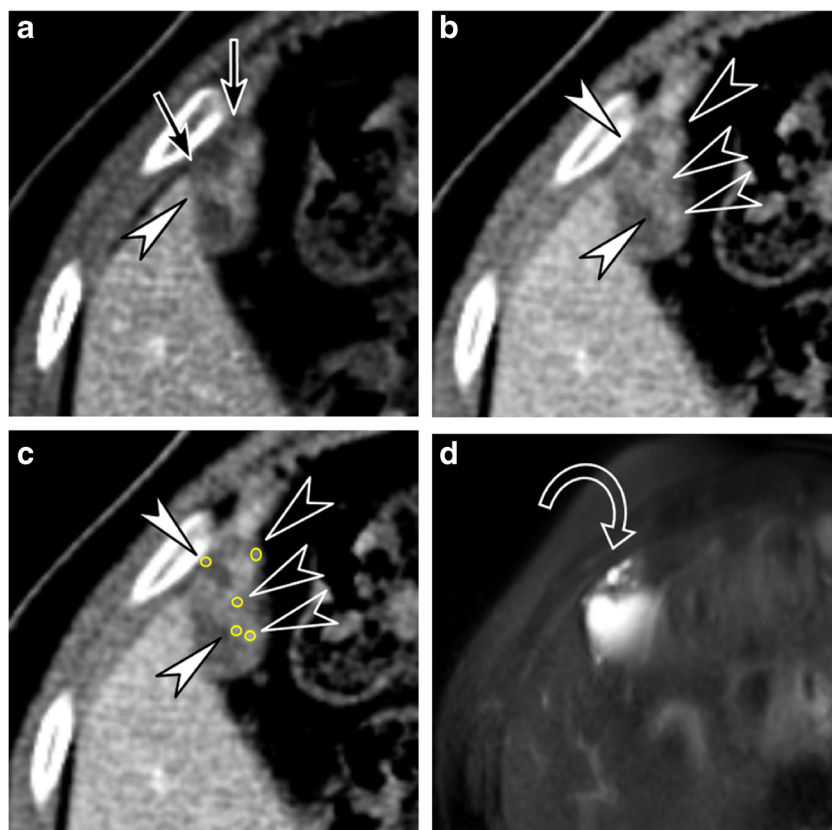
Other differentiating benign CT features of GBWT

Contour of GBWTs Smoothness of the mucosa was significantly more frequent in the benign GBWT group on CT. The three readers showed moderate to substantial agreement for mucosal smoothness (0.58–0.71) (Table 3).

Enhancing characteristics of GBWTs Double-layering enhancement and an enhancement degree weaker than the renal cortex were significantly more frequent in the benign GBWT group on CT. The three readers showed fair to moderate agreements for the layered pattern (0.21–0.41) and fair to substantial agreements for the enhancement degree (0.25–0.72) (Table 3).

Combined CT findings in GBWTs When at least two of four criteria, i.e., the positive cotton ball sign on PVP, smooth mucosal contour, double-layer enhancement, and enhancement degree weaker than the renal cortex on PVP, were used in combination, the sensitivity and specificity for differentiating benign from malignant or premalignant GBWT were 90% (57/63) and 74% (32/43). When all the four findings were present, a specificity of 98% (42/43) was achieved (Table 4). On multivariate regression analysis, the first and second most predictive CT findings of benignity were smoothness of the mucosa (odds ratio: 28.6, 95% confidence interval: 6.9–118.9) and an enhancement degree weaker than the renal cortex (odds ratio: 13.6, 95% confidence interval: 1.7–111.2) ($p < 0.05$).

Table 1 Prevalence of the cotton ball sign and pearl necklace sign in each of three subgroups of GBWTs

	Benign		Malignant or premalignant ($n = 43$)	p value[*]
	GA ($n = 34$)	Other benign ($n = 29$)		
Cotton ball sign on PVP CT	25 (74%)	16 (55%)	6 (14%)	< 0.01
Pearl necklace sign on T2WI and MRCP	15 (44%)	10 (34%)	1 (2%)	< 0.01

Note. Data are numbers of GBWTs with percentages in parentheses

[*] p value was calculated with chi-square test

GBWT = gallbladder wall thickening; GA = gallbladder adenomyomatosis; PVP = portal venous phase; CT = computed tomography; T2WI = T2-weighted image; MRCP = magnetic resonance cholangiopancreatography

Table 2 Sensitivity, specificity, and accuracy of the cotton ball sign and pearl necklace sign in differentiating GA from malignancy or premalignancy

	Sensitivity[a]		Specificity[b]		Accuracy[c]	
	Percentage[d]	Numerator/ denominator	Percentage[d]	Numerator/ denominator	Percentage[d]	Numerator/ denominator
Cotton ball sign on PVP CT	74 (48, 100)	25/34	86 (61, 100)	37/43	81 (62, 100)	62/77
Pearl necklace sign on T2WI or MRCP	44 (25, 73)	15/34	98 (70, 100)	42/43	74 (56, 96)	57/77
p value[*]	0.02		0.06		-	

Note. [a] Sensitivity of cotton ball sign (%) = (GA with a positive cotton ball sign/total of 34 GAs) × 100. Sensitivity of pearl necklace sign (%) = (GA with a positive pearl necklace sign/total of 34 GAs) × 100

[b] Specificity of cotton ball sign (%) = (Malignant or premalignant GBWT with a negative cotton ball sign/total of 43 malignancies or premalignancies) × 100. Specificity of the pearl necklace sign (%) = (Malignant or premalignant GBWT with a negative pearl necklace sign/total of 43 malignancies or premalignancies) ×100

[c] Accuracy of the cotton ball sign (%) = (GA with a positive cotton ball sign + malignant or premalignant GBWT with a negative cotton ball sign)/(total of 77 GAs or malignancies or premalignances) × 100. Accuracy of pearl necklace sign (%) = (GA with a positive pearl necklace sign + malignant or premalignant GBWT with a negative pearl necklace sign)/(total of 77 GAs or malignancies or premalignancies) × 100

[d] Data in parentheses are 95% confidence intervals

[*] *p* value was calculated with McNemar's test

GA = gallbladder adenomyomatosis; PVP = portal venous phase; CT = computed tomography; T2WI = T2-weighted image; MRCP = magnetic resonance cholangiopancreatography; GBWT = gallbladder wall thickening

Discussion

Our study demonstrated that the "cotton ball" sign on CE-CT may be utilised as an imaging sign of GA at CE-CT. Prevalence of the cotton ball sign on CE-CT in three subgroups of GBWTs, i.e., GA, other benign, and malignant or premalignant groups, showed a similar pattern to that of pearl necklace sign, which is significantly higher in GA than in a malignant or premalignant group. Furthermore, the cotton ball sign at CT provided higher sensitivity and comparable specificity in diagnosing GA compared with the pearl necklace sign at MR imaging. With the widespread use of CT for evaluation of abdominal symptoms,

Table 3 Differences in CT imaging features between benign and malignant or premalignant GBWTs

	Benign (*n* = 63)	Malignant or premalignant (*n* = 43)	*p* value[*]	Weighted kappa statistics		
				Readers 1 and 2	Readers 2 and 3	Readers 3 and 1
Cotton ball sign on PVP			< 0.01	0.56	0.43	0.39
Present	41 (65%)	6 (14%)				
Absent	22 (35%)	37 (86%)				
Mucosal smoothness			< 0.01	0.58	0.68	0.71
Smooth	53 (84%)	6 (14%)				
Irregular	10 (16%)	37 (86%)				
Layered pattern on PVP			< 0.01	0.32	0.21	0.41
Double layer	45 (71%)	8 (19%)				
Single layer	18 (29%)	35 (81%)				
Enhancement degree on PVP			< 0.01	0.25	0.43	0.72
Weaker than renal cortex	60 (95%)	33 (77%)				
Similar to or stronger than renal cortex	3 (5%)	10 (23%)				
Pericholecystic infiltration			0.15	0.35	0.32	0.51
Present	17 (27%)	6 (14%)				
Absent	46 (73%)	37 (86%)				

Note. Data are numbers of GBWTs with percentages in parentheses

[*] *p* value was calculated with Fisher's exact test

CT = computed tomography; GBWT = gallbladder wall thickening; PVP = portal venous phase

Table 4 Combined CT findings in GBWTs

No. of CT findings	Benign (n = 63)	Malignant or premalignant (n = 43)
1	63 (100%)	36 (84%)
2	57 (90%)	11 (26%)
3	48 (76%)	5 (12%)
4	31 (49%)	1 (2%)

Note. Data are numbers of GBWTs with one or more of the following findings at CT: positive cotton ball sign on PVP, smooth mucosal contour, double layer enhancement, and enhancement degree weaker than the renal cortex on PVP

CT = computed tomography; GBWT = gallbladder wall thickening; PVP = portal venous phase

radiologists frequently encounter incidental GBWT at CT and a considerable portion of such cases may become a diagnostic dilemma owing to the similarity in appearance of GA and GB cancer on CT. As for the patients, they may undergo unnecessary cholecystectomy in fear of early GB cancer [3, 25]. As GAs are generally asymptomatic and benign, making the correct diagnosis is important to prevent misinterpretation as GB cancer leading to incorrect treatment [18]. Additionally, immediate characterisation of incidental GA with CE-CT utilising the cotton ball sign may obviate referrals and further imaging, while reducing patient anxiety.

Traditionally, the radiological diagnosis of GA has been largely dependent on visualising RAS in the GBWT, presenting as an intramural cyst with the comet-tail artefact or twinkling artefact on US, the pearl necklace sign at MRCP, and the rosary sign and multiple intramural cysts on CT [7, 15–18]. While US is widely accepted as the primary imaging technique for GB disease [20, 25], in some cases there may be some limitations in US, as dilated RAS can show variable echogenicity, depending on the materials accumulated in the RAS [3]. In some cases, US may be partially limited because of operator dependency, artefacts such as reverberation, and inadequate GB visualisation in obese patients resulting from sonic attenuation [3]. Considering that CT is relatively less affected by obesity compared with US and has wider availability and lower cost than MR [3, 26], CT has its own advantage as a diagnostic modality for GBWT. However, according to previous literature that addressed the differentiation of GA from GB cancer on CT [9], sensitivity

Fig. 5 A 44-year-old female, pathologically proven underlying GA in the GB fundus and co-existing intra-cystic papillary neoplasm with associated invasive carcinoma in the body. **A** Portal venous phase transverse CT image shows focal thickening of the GB wall with outer border (*arrowheads*), "cotton ball sign" in the fundus. **B** On T2WI of the same patient, the pearl necklace sign (*curved arrow*) is noted in the fundus. **C** Portal venous phase coronal CT image shows irregular wall thickening of the single layer enhancement pattern in the GB body favouring malignancy. **D** Surgical specimen of the GB. **E** Photomicrograph shows underlying GA and papillary neoplasm. (Haematoxylin-eosin stain; original magnification ×10). GA = gallbladder adenomyomatosis; GB = gallbladder
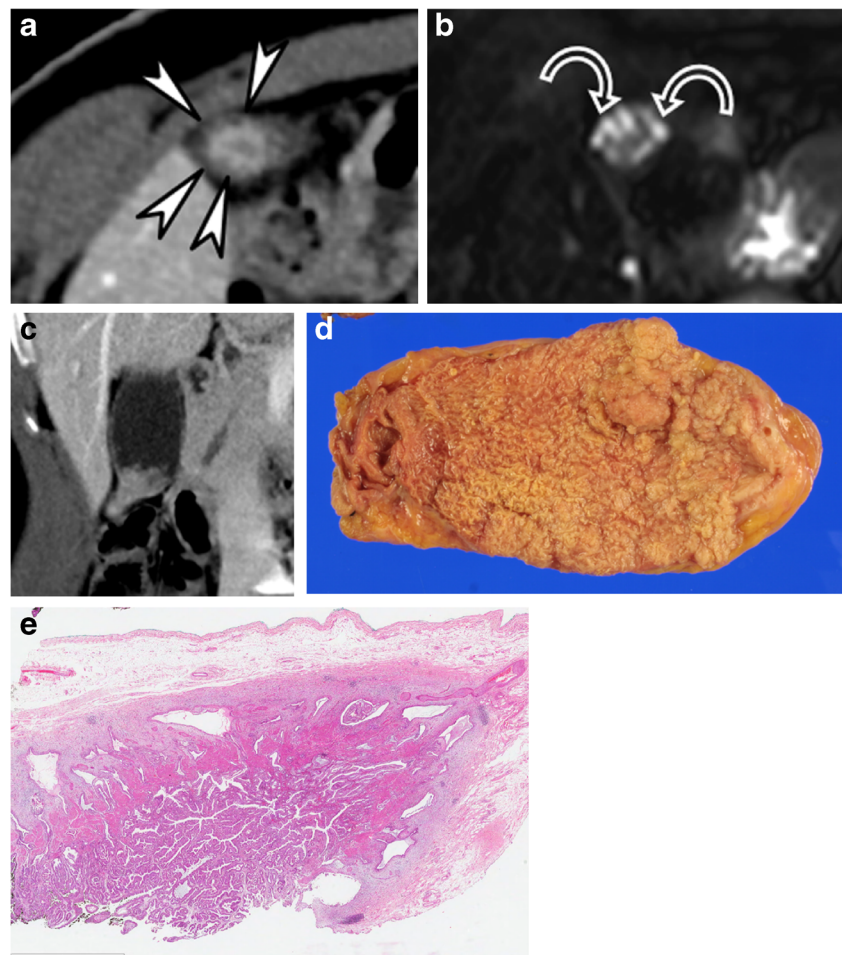
for diagnosing GA on CT using intramural diverticuli or the "rosary" sign was 36%, which is relatively low. It could be attributed to the fact that small or collapsed RAS may not be evidently visualised as the "rosary sign" [2, 3] and limited soft tissue contrast of CT in revealing small RAS. However, our results demonstrated that the cotton ball sign at CE-CT provided significantly higher sensitivity than the pearl neckace sign at MR while maintaining similar specificity in differentiating GA from GB cancer. Taking into account these findings, we postulate that the cotton ball sign represents enhancement of the proliferated lining mucosa of multiple small or collapsed RASs and thus is an extended version of intramural diverticula on CT for small or collapsed RAS in GA. Therefore, it could be used to enhance the diagnostic performance of MDCT and confidence in diagnosing benign GBWT.

An interesting point is that six malignant GBWTs showed a positive cotton ball sign on CE-CT in our study. One case was an intracystic papillary neoplasm with associated invasive carcinoma, which infiltrated into the co-existing underlying GA (Fig. 5); one was adenocarcinoma with cystic changes of the tumour glands and co-existing GA; two were adenocarcinomas that showed cystic change with pseudo-invasion; one was well-differentiated adenocarcinoma with cystic changes of the tumour glands; the remaining one was moderately differentiated adenocarcinoma that did not show cystic change, but rather abundant neutrophilic infiltration suggesting the possibility of micro-abscesses. Our study results are quite similar to those of a previous study that reported GB cancer coexisting with GA [27] and to another study reporting that 8.6% of well-differentiated GB cancers with mucin production (3/35) had cystic components and therefore mimicked adenomyomatosis at MR imaging [28]. Until now, the presence of fluid-filled RAS within the GBWT, which can be depicted as the pearl necklace sign at MR or the rosary sign at CT, has been widely accepted as being specific to a GA diagnosis [3, 10, 11]. However, GB cancer with cystic change of the tumour gland or mucin may show similar imaging features [28]. Similarly, application of the cotton ball sign at CT requires special caution as well-differentiated or mucinous adenocarcinomas may show glandular proliferation as well as cystic components in the GBWT. Considering that there were malignant GBWTs showing the cotton ball sign, we recommend a combined interpretation of the this sign with other imaging features such as the pattern and degree of enhancement of the GB wall at CE-CT for more reliable differentiation of benign from malignant GBWT, as when all the four findings were present in our study, a specificity of 98% (42/43) was achieved.

Our study has limitations. First, as we limited our study population to those whom had undergone preoperative CT and MR followed by cholecystectomy, there may have been selection bias. However, such selection bias is inevitable in a retrospective design, and our results may provide useful information when preoperative diagnosis is challenging and

cholecystectomy is considered rather than when a GBWT appears confidently benign. Second, in our study, 55% (16/29) of benign GBWTs without pathologically identified GA or RAS in our study showed the cotton ball sign and 34% (10/29) showed the pearl necklace signs. This could be attributed to the fact that specimens of the benign GB disease were not completely included in the histological slide production. Therefore, there may be a tendency toward under-reporting GA in pathology examinations, and some true GAs may have been categorised into the other benign entity group in our study. Third, we could not perform pathological-radiological correlation for the entire study sample regarding the cotton ball sign because of the retrospective design. Last, we could not analyse the ultrasound findings in comparison with CT and MRI findings. Due to our retrospective design, not every patient underwent an ultrasound examination for GB abnormality. Further study regarding the correlation between the cotton ball sign and conventional ultrasound findings such as intramural cysts indicating RAS, intramural echogenic spots representing intramural calcification, or cholesterol deposits in the RAS [15, 29–32] may offer useful information.

In conclusion, the cotton ball sign on CE-CT was helpful in differentiating GA from malignancy for focal or diffuse GBWT with higher sensitivity and comparable specificity to those of the pearl necklace sign.

Compliance with ethical standards

References

1. Kim SJ, Lee JM, Lee JY et al (2008) Analysis of enhancement pattern of flat gallbladder wall thickening on MDCT to differentiate gallbladder cancer from cholecystitis. AJR Am J Roentgenol 191:765–771

2. Bonatti M, Vezzali N, Lombardo F et al (2017) Gallbladder adenomyomatosis: imaging findings, tricks and pitfalls. Insights Imaging 8:243–253

3. Hammad AY, Miura JT, Turaga KK, Johnston FM, Hohenwalter MD, Gamblin TC (2016) A literature review of radiological findings to guide the diagnosis of gallbladder adenomyomatosis. HPB (Oxford) 18:129–135

4. Kim JH, Jeong IH, Han JH et al (2010) Clinical/pathological analysis of gallbladder adenomyomatosis; type and pathogenesis. Hepatogastroenterology 57:420–425

5. Cariati A, Cetta F (2003) Rokitansky-Aschoff sinuses of the gallbladder are associated with black pigment gallstone formation: a scanning electron microscopy study. Ultrastruct Pathol 27:265–270

6. Mariani PJ, Hsue A (2011) Adenomyomatosis of the gallbladder: the "good omen" comet. J Emerg Med 40:415–418

7. Joo I, Lee JY, Kim JH et al (2013) Differentiation of adenomyomatosis of the gallbladder from early-stage, wall-thickening-type gallbladder cancer using high-resolution ultrasound. Eur Radiol 23:730–738

8. Chantarojanasiri T, Hirooka Y, Kawashima H, Ohno E, Kongkam P, Goto H (2017) The role of endoscopic ultrasound in the diagnosis of gallbladder diseases. J Med Ultrason (2001) 44:63–70

9. Ching BH, Yeh BM, Westphalen AC, Joe BN, Qayyum A, Coakley FV (2007) CT differentiation of adenomyomatosis and gallbladder cancer. AJR Am J Roentgenol 189:62–66

10. Yoshimitsu K, Honda H, Jimi M et al (1999) MR diagnosis of adenomyomatosis of the gallbladder and differentiation from gallbladder carcinoma: importance of showing Rokitansky-Aschoff sinuses. AJR Am J Roentgenol 172:1535–1540

11. Haradome H, Ichikawa T, Sou H et al (2003) The pearl necklace sign: an imaging sign of adenomyomatosis of the gallbladder at MR cholangiopancreatography. Radiology 227:80–88

12. Mirbagheri SA, Mohamadnejad M, Nasiri J, Vahid AA, Ghadimi R, Malekzadeh R (2005) Prospective evaluation of endoscopic ultrasonography in the diagnosis of biliary microlithiasis in patients with normal transabdominal ultrasonography. J Gastrointest Surg 9:961–964

13. Imazu H, Mori N, Kanazawa K et al (2014) Contrast-enhanced harmonic endoscopic ultrasonography in the differential diagnosis of gallbladder wall thickening. Dig Dis Sci 59:1909–1916

14. Miyazaki T, Yamashita Y, Tsuchigame T, Yamamoto H, Urata J, Takahashi M (1996) MR cholangiopancreatography using HASTE (half-Fourier acquisition single-shot turbo spin-echo) sequences. AJR Am J Roentgenol 166:1297–1303

15. Hwang JI, Chou YH, Tsay SH et al (1998) Radiologic and pathologic correlation of adenomyomatosis of the gallbladder. Abdom Imaging 23:73–77

16. Clouston JE, Thorpe RJ (1991) Case report–CT findings in adenomyomatosis of the gallbladder. Australas Radiol 35:86–87

17. Chao C, Hsiao HC, Wu CS, Wang KC (1992) Computed tomographic finding in adenomyomatosis of the gallbladder. J Formos Med Assoc 91:467–469

18. Stunell H, Buckley O, Geoghegan T, O'Brien J, Ward E, Torreggiani W (2008) Imaging of adenomyomatosis of the gall bladder. J Med Imaging Radiat Oncol 52:109–117

19. Altman DG (1990) Practical statistics for medical research. CRC press

20. van Breda Vriesman AC, Engelbrecht MR, Smithuis RH, Puylaert JB (2007) Diffuse gallbladder wall thickening: differential diagnosis. AJR Am J Roentgenol 188:495–501

21. Levy AD, Murakata LA, Rohrmann CA Jr (2001) Gallbladder carcinoma: radiologic-pathologic correlation. Radiographics 21:295–314 questionnaire, 549-255

22. Baron RL (1991) Computed tomography of the biliary tree. Radiol Clin North Am 29:1235–1250

23. Zissin R, Osadchy A, Shapiro-Feinberg M, Gayer G (2003) CT of a thickened-wall gall bladder. Br J Radiol 76:137–143

24. Westra WH (2003) Surgical pathology dissection: an illustrated guide, 2nd edn. Springer, New York

25. Bang SH, Lee JY, Woo H et al (2014) Differentiating between adenomyomatosis and gallbladder cancer: revisiting a comparative study of high-resolution ultrasound, multidetector CT, and MR imaging. Korean J Radiol 15:226–234

26. Adusumilli S, Siegelman ES (2002) MR imaging of the gallbladder. Magn Reson Imaging Clin N Am 10:165–184

27. Imai H, Osada S, Sasaki Y et al (2011) Gallbladder adenocarcinoma with extended intramural spread in adenomyomatosis of the gallbladder with the pearl necklace sign. Am Surg 77:E57–E58

28. Yoshimitsu K, Irie H, Aibe H et al (2005) Well-differentiated adenocarcinoma of the gallbladder with intratumoral cystic components due to abundant mucin production: a mimicker of adenomyomatosis. Eur Radiol 15:229–233

29. Rice J, Sauerbrei EE, Semogas P, Cooperberg PL, Burhenne HJ (1981) Sonographic appearance of adenomyomatosis of the gallbladder. J Clin Ultrasound 9:336–337

30. Raghavendra BN, Subramanyam BR, Balthazar EJ, Horii SC, Megibow AJ, Hilton S (1983) Sonography of adenomyomatosis of the gallbladder: radiologic-pathologic correlation. Radiology 146:747–752

31. Brambs HJ, Wrazidlo W, Schilling H (1990) The sonographic image of gallbladder adenomyomatosis. Rofo 153:633–636

32. Boscak AR, Al-Hawary M, Ramsburgh SR (2006) Best cases from the AFIP: Adenomyomatosis of the gallbladder. Radiographics 26:941–946